Particle-core coupling in ^{141}Pm

E. Gülmez,* M. W. Drigert,† and J. A. Cizewski‡
A.W. Wright Nuclear Structure Laboratory, Yale University, New Haven, Connecticut 06511
(Received 28 November 1988)

The high angular momentum structure of ^{141}Pm has been studied via the ^{126}Te(^{19}F,4$n\gamma$) reaction at beam energies from 74 to 84 MeV. In-beam γ-ray spectroscopy techniques, including γ-ray excitation function, γ-γ coincidence, and γ-ray angular distribution measurements were used. A level spectrum up to an excitation energy of 4782 keV was constructed. Definite parity assignments were made up to the $\frac{21}{2}^-$ state. The low-lying structure is discussed in terms of a weak coupling between the valence proton and the $N=80$ cores. The earlier treatment of ^{141}Pm in terms of a particle-plus-triaxial rotor is critiqued.

I. INTRODUCTION

Recent measurements[1] on neutron-deficient $A\approx 130$ nuclei with heavy-ion fusion-evaporation reactions have identified a new region of deformation. The results of these experiments done at the Daresbury Nuclear Structure Facility can be well reproduced by the theoretical calculations by Leander and Möller[2] where deformations $\beta\geq 0.3$ were predicted. On the other hand, there are relatively little data at high angular momentum on the transitional nuclei with $N<82$ near $Z=64$. The present work on ^{141}Pm is our second study of $N=80$ nuclei at moderately high angular momentum; we have previously reported measurements[3] on ^{140}Nd.

The low-lying excited states in ^{141}Pm were first studied[4] by measuring the γ rays and internal conversion electrons following the β^+ decay of ^{141}Sm. Many excited levels below 3 MeV in excitation in ^{141}Pm were identified, but few spin parity assignments were made. The first in-beam study of ^{141}Pm was carried out by Piiparinen, *et al.*[5] In this measurement the excited levels in ^{141}Pm were populated via the ^{142}Nd(p,2$n\gamma$), ^{141}Pr(^{3}He,3$n\gamma$), and ^{141}Pr(α,4$n\gamma$) reactions. States of up to moderate angular momentum were identified by utilizing standard γ-ray spectroscopy techniques, including delayed and prompt γ-γ coincidence, angular distribution, excitation function, and internal conversion electron measurements. A level scheme up to $E_x\approx 2.6$ MeV and $J^\pi=\frac{17}{2}^+$ was established. The ^{142}Nd(p,2$n\gamma$) and ^{141}Pr(α,4$n\gamma$) measurements were repeated and reported more recently by Aryaeinejad *et al.*[6]. Although a lower beam energy was used in this (α,4$n\gamma$) reaction study, a level scheme up to $E_x\approx 3$ MeV was established. The lifetime of the $\frac{11}{2}^-$ isomeric state at 628.5 keV has been measured in all the previous works;[4-6] Refs. 5 and 6 have obtained half-life values of 0.59(2) μs and 0.63(2) μs, respectively.

In order to establish better the higher angular momentum structure of the transitional nuclei below ^{146}Gd, and to probe the onset of deformation in this region, we have studied ^{141}Pm via the ^{126}Te(^{19}F,4$n\gamma$) reaction. The results of these measurements are reported in the present paper and are examined in terms of a simple weak coupling model.

II. EXPERIMENTAL PROCEDURE AND MEASUREMENTS

The high angular momentum states in the ^{141}Pm nucleus were populated via the ^{126}Te(^{19}F,4$n\gamma$) reaction. The ^{19}F beam was produced at the Yale MP-1 tandem Van de Graaff accelerator. An ≈ 1 mg/cm^2 ^{126}Te target was used in the measurements. The target was produced by evaporating isotopically enriched ^{126}Te onto an ≈ 10 mg/cm^2 gold foil. In all of the measurements, the ^{19}F beam was completely stopped in the target assembly by a thick natural lead foil behind the gold backed target.

The γ-ray deexcitation of the levels populated in the ^{126}Te+^{19}F reaction was studied by using standard γ-ray spectroscopy techniques, including excitation function, angular distribution and γ-γ coincidence measurements with three Ge detectors: An n-type high purity germanium coaxial "gamma-x" detector with an efficiency of $\approx 25\%$; a Ge(Li) detector with an efficiency of 20%; and a 12% Ge(Li) detector. [All efficiencies are relative to a 7.6 cm×7.6 cm NaI(Tl) scintillator.] Typical energy resolutions of these detectors for our measurements were 2.7, 2.2, and 2.7 keV full width at half maximum (FWHM), respectively, at 1332 keV.

An excitation function measurement was performed over a beam energy range of 74–84 MeV with 2 MeV increments. The results for strong lines in ^{140}Nd and ^{141}Pm are summarized in Fig. 1 and compared with predictions from the program SPIT (Ref. 7). The yields of specific γ rays as a function of beam energy were normalized by the Coulomb excitation lines of the target, the beam, and the gold backing. Based on the yields of several prominent lines in ^{141}Pm, the 78 MeV ^{19}F beam energy was determined to be the optimum energy for populating the states of interest.

In the γ-γ coincidence measurement coincident γ-ray pairs from the three Ge detectors placed at 0°, −90°, and 90° were recorded on magnetic tapes for later analysis. An electronic time resolution of 13–15 ns was obtained, depending on detector pair combination. No evidence for delayed coincidences was observed in any time spectrum. Figure 2 shows the total coincident γ-ray spectrum. Several gated spectra are given in Figs. 3 and 4.

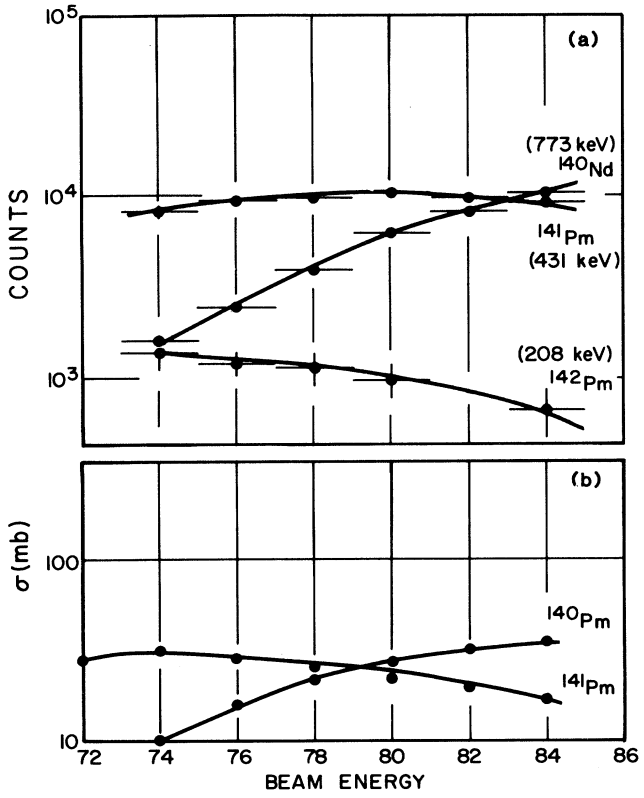

FIG. 1. Comparison of experimental and theoretical (SPIT, Ref. 7) excitation functions for the $^{19}F+^{126}Te$ reaction. In (a) the yields (in arbitrary units) of the gamma rays associated with the $3n$, $4n$, and $4np$ channels are indicated. The population of ^{140}Nd is actually a combination of the $4np$ channel and, predominantly, the β^+ decay of the $5n$ channel. The predicted excitation functions are given in (b); the predictions for the $3n$ channel are much smaller than the observations.

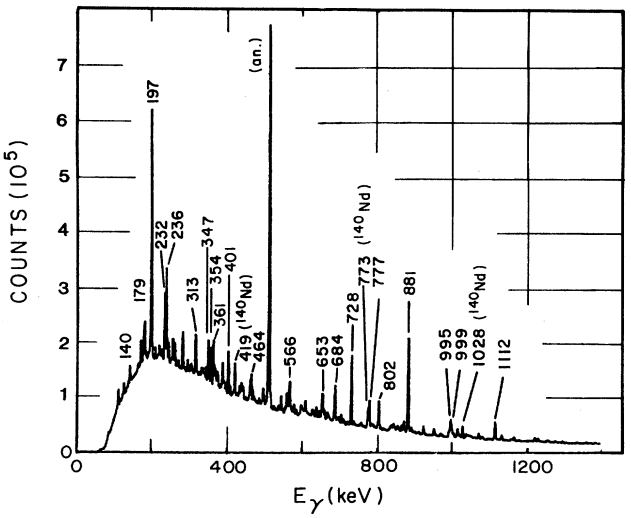

FIG. 2. Total spectrum of coincident gamma rays observed in the $^{19}F+^{126}Te$ reaction.

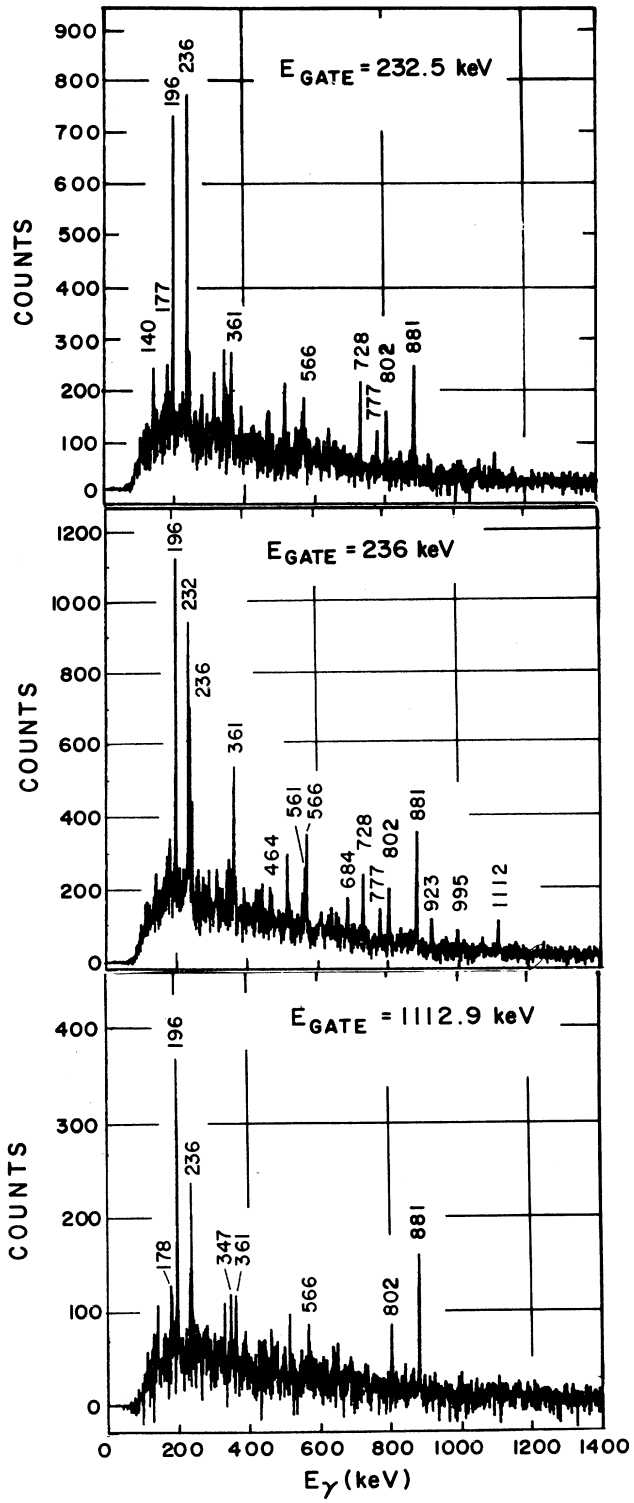

FIG. 3. Background subtracted γ-γ coincidence spectra obtained when gating on the 232.5, 236, and 1112 keV transitions in ^{141}Pm.

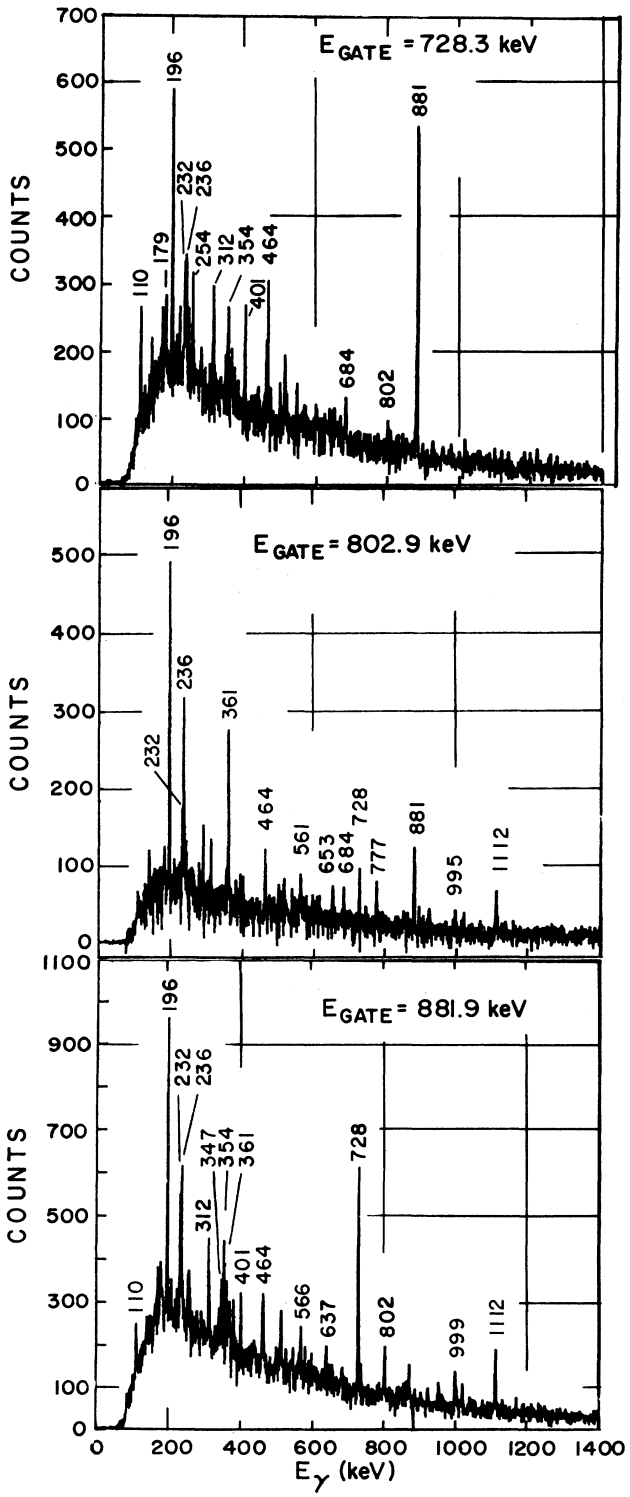

FIG. 4. Background subtracted γ-γ coincidence spectra obtained when gating on the 728, 802, and 881 keV transitions in ^{141}Pm.

The angular distributions of the γ rays produced in the ^{126}Te+^{19}F reaction were measured with an 80 MeV ^{19}F beam. This slightly higher beam energy was chosen to populate better the higher angular momentum states. Data were collected from 0° to 90°, with respect to the beam, in 15° increments. The normalization of the data at different angles was made possible by a monitor detector placed at −90°. The efficiency of the detector was measured at each angle by using a ^{152}Eu γ-ray source placed in the target position. After normalization and corrections for the efficiency as a function of angle, the data were fitted to a fourth-order truncated Legendre polynomial to extract the intensities, I_γ, and A_2 and A_4 coefficients which were used in the determination of the multipolarities of the transitions. Intensities and the angular distribution coefficients, corrected for finite solid angle effects, for transitions in ^{141}Pm are listed in Tables I and II. Further details of the analysis are presented in Ref. 8.

III. LEVEL SPECTRUM

The level spectrum of ^{141}Pm deduced from the ^{126}Te(^{19}F,4$n\gamma$) reaction is presented in Fig. 5. A total of 36 γ-ray transitions was placed. Preliminary results have been presented in Refs. 8 and 9. The spin-parities of the $\frac{5}{2}^+$ ground state and $\frac{7}{2}^+$ and $\frac{11}{2}^-$ states and the lifetime of the $\frac{11}{2}^-$ isomeric state were taken from the previous measurements,[5,6] as were the energies and multipolarities of the low-lying transitions of 196.9, 628, and 431 keV.

As seen in Tables I and II, the angular distribution coefficients were not sufficiently well established to make definite spin-parity assignments in most cases and to extract the mixing ratios in general. Another difficulty in making spin-parity assignments for the levels above the state at E_x=2623.3 keV arises because of the 236 keV doublet and the ≈197 keV triplet lines. The angular distribution coefficients for the 236 keV unresolved doublet are consistent with a $\Delta J=1$ transition. However, since the 236 keV transition is a doublet, no definite multipolarity can be assigned and, therefore, the spin assigned to the state at 2859 keV is tentative. (The energies for the components of the 236 keV multiplet were taken from coincidence spectra.) Because the 196.5 keV γ-ray transition placed above the E_x=2859 keV level is part of a triplet and is obscured by the strong Coulomb excitation line from the ^{19}F beam, determining the multipolarity of the 196.5 keV transition and the spin-parities of the levels above the E_x=2859 keV level are not possible.

Two of the three ≈197 keV γ-ray transitions in the deexcitation spectrum of ^{141}Pm in Fig. 5 were observed previously.[5,6] Our measurements indicated a third ≈197 keV γ-ray transition, which we have placed above the 2859 keV level. This placement is supported by the prompt coincidences between, for example, the 881 and 197 keV transitions, which could not be understood with the previously placed[5,6] ≈197 keV γ-ray transitions: The 197.7 keV transition parallel to the 881 keV transition, and the 196.6 keV transition below the $\frac{11}{2}^-$ 0.59 μs isomeric state at 628.5 keV. In order to solve this mystery the coincidence spectrum gated on the 197 keV peak

was regenerated as six separate spectra, each coincident with different parts of the 197 keV peak. Three of these spectra, a low-energy part, a middle part and a high-energy part are compared in Fig. 6. As seen in this figure, the relative peak heights of the 431 and 881 keV γ-ray transitions, for example, are not the same in these three spectra. On the low-energy side they are comparable, while on the high-energy side the 431 keV γ-ray transition is the dominant transition, as expected for the coincident spectrum gated on the 197 keV ground-state transition. These results support the current placement of a ≈ 196.5 keV γ-ray transition above the $E_x = 2859$ keV level. The transition energy of this third ≈ 197 keV γ-ray transition was estimated from the spectrum gated on the 881 keV line, which sees only this third ≈ 197 keV transition. The energies of the previously observed ≈ 197 keV transitions were taken from earlier measurements which did not have a strong contamination from the ≈ 197 keV transition from the Coulomb excitation of the beam.

TABLE I. Angular distribution coefficients for gamma rays assigned to ^{141}Pm as observed in the ^{19}F+^{126}Te reaction.[a]

E_γ (keV)[b]	A_2/A_0[c]	A_4/A_0[c]
109.98(10)	0.23(4)	−0.16(4)
140.00(13)	1.1(8)	0.27(7)
169.6(2)	−0.31(11)	−0.05(12)
177.3(3)	−0.23(13)	−0.01(15)
179.3(2)	−0.35(10)	0.01(11)
232.49(11)	−0.25(6)	−0.14(6)
236.41(10)	−0.20(4)	0.02(4)
254.5(3)	−0.38(11)	0.21(14)
258.1(2)	−0.20(12)	0.04(14)
260.0(3)	0.03(15)	−0.28(14)
312.6(3)	−0.50(18)	−0.23(18)
314.0(5)	−0.47(22)	0.27(22)
347.09(13)	−0.20(5)	−0.08(6)
354.9(5)	−0.85(15)	0.01(16)
361.14(13)	−0.34(5)	−0.10(6)
401.65(10)[d]	−0.31(3)	0.03(3)
431.56(7)	−0.02(1)	−0.08(2)
461.4(2)[d]	−0.08(13)	−0.06(15)
464.21(12)	−0.25(7)	−0.08(8)
496.49(14)	−0.21(8)	−0.16(10)
562.0(3)	−0.95(10)	0.18(12)
566.07(14)	−0.54(5)	0.02(6)
608.3(2)	0.53(10)	0.07(9)
628.5(2)	0.13(8)	−0.15(9)
637.8(2)	−0.10(6)	−0.18(7)
651.1(2)	0.61(10)	−0.49(10)
653.3(2)	−0.72(7)	0.16(9)
682.1(2)	0.28(7)	−0.11(8)
684.25(13)	−0.86(5)	0.08(6)
701.3(2)	−0.52(13)	0.21(15)
728.30(7)	0.29(2)	−0.08(2)
777.02(6)	0.38(3)	−0.11(4)
802.89(8)	−0.02(2)	0.08(3)
871.22(14)	0.06(6)	−0.06(7)
881.90(6)	0.29(1)	−0.06(1)
923.2(3)	−0.06(37)	0.43(44)
951.8(3)	0.63(18)	−0.25(17)
995.77(11)	0.31(4)	−0.10(4)
999.09(13)	0.34(5)	−0.11(5)
1068.2(2)	0.15(14)	0.06(14)
1112.85(10)	−0.35(3)	0.02(3)
1163.8(2)	−0.05(11)	−0.02(12)

[a]Transitions obscured by Coulomb excitation lines are not included.

[b]Errors on the last digit are a combination of uncertainties coming from peak fitting and energy calibration of the spectrum.

[c]Errors on the last digits are a combination of propagated uncertainties of the peak areas, uncertainties in fitting, and finite angle corrections.

[d]This line is partly obscured by a strong contribution from another channel.

The 401 keV transition has been placed between the 2640 and 2238 keV levels. However, this line is obscured by a strong contaminant from another reaction channel. Excitation functions for the 401 and 386 keV lines, the latter the strongest line in the spectrum gated on the 401 keV transition, give higher yields at beam energies higher than the optimum beam energy for the $4n$(^{141}Pm) channel.[8] Hence, the 123, 373, 386, 401, 564, and 755 keV lines, which are in prompt coincidence with each other, are in a cascade that probably belongs to the $5n$(^{140}Pm) channel.

The main complication in the deexcitation of ^{141}Pm occurs in the prompt coincidences between the 464 and/or 728 keV transitions and the transitions above the $E_x = 2859$ keV level, such as the 802 keV γ-ray transition. From the γ-γ coincidence spectra, it is clear that the connection(s) between the 2859 keV or higher levels and the 728 and/or 881 keV lines are made by mainly the 140, 177, and 291 keV lines and some low-energy transitions not observed by our detectors. One possible scenario for connecting the 728 and/or 881 keV lines and the levels above 2859 keV could involve a very low energy, totally converted transition populating a state either around ≈ 2840 or ≈ 3050 keV followed by several separate cascades of mostly low-energy γ-ray transitions, including the 140, 177, and 291 keV lines. Should there be an isomeric state involved in this scenario, it must have a lifetime less than 10–20 ns because of the prompt coincidences observed between the 728 and/or 881 transitions and the lines above the 2859 keV level. For the above reasons and the low statistics in the relevant gated spectra, we were unable to place these lines unambiguously in the level spectrum in Fig. 5. To solve this problem would require additional measurements, possibly with a planar, low-energy detector.

There is also a clear prompt coincidence between the 802 and 1019 keV transitions which might be possible via a weak 525 keV transition between the 3056 and 2509 keV levels. We see such a weak line in the coincidence spectrum gated on the 881 keV transitions. However, because of the poor statistics, we are not sure that this is the same line in the spectrum gated on the 802 keV transitions. Spectra gated on the 524 and 1019 keV transitions were not helpful because of poor statistics. Also, the 179 keV transition is in prompt coincidence with the ≈ 197, 312, 728, and 881 keV lines, which indicates that

TABLE II. Gamma rays observed in ^{141}Pm via the ^{19}F+^{126}Te reaction.[a]

E_γ(keV)[b]	Placement	I_γ^c	Character[d]
109.98(10)	2661–2551		$E2$
140.00(13)		462(97)	
169.6(2)		207(43)	
177.3(3)		214(46)	
179.3(2)		268(53)	
196.5	3056–2859		
196.9	196–0		$M1$[e]
197.7	1510–1312		
232.49(11)	4452–4220	168(24)	
236.41(10)	2859–2623 3859–3622	246(33)	
254.5(3)		100(16)	
258.1(2)	2640–2381	86(15)	
260.0(3)	1572–1312	75(14)	
291.6(3)			
312.6(3)	2551–2238	106(20)	
314.0(5)		81(17)	
347.09(13)	3403–3056	247(22)	
354.9(5)		144(17)	
361.14(13)	4220–3859	179(16)	
401.65(10)	2640–2238	60(30)[f]	
431.56(7)	628–196	≡1000	$M2$[e]
461.4(2)		78(11)	
464.21(12)	2702–2238	113(12)	$M1+E2$
496.49(14)	3047–2551	89(10)	
562.0(3)	4782–4220	72(11)	
566.07(14)	3622–3056	195(22)	
608.3(2)	2622–2014	105(13)	
628.5(2)	628–0	122(17)	$E3$[e]
637.8(2)	4041–3403	135(16)	
651.1(2)		84(13)	
653.3(2)	2623–1969	114(15)	$M1+E2$
682.1(2)		101(13)	
684.25(13)	1312–628	239(26)	$M1+E2$
701.3(2)	2014–1312	62(10)	
728.30(7)	2238–1510	554(54)	$E2$
777.02(6)	973–196	218(24)	$E2$
802.89(8)	3859–3056	332(34)	
871.22(14)	2381–1510	129(16)	
881.90(6)	1510–628	993(100)	$E2$
923.2(3)	4782–3859	28(7)	
951.8(3)		62(11)	
995.77(11)	1969–973	157(19)	$E2$
999.09(13)	2509–1510	117(15)	$E2$
1019.9(3)	2530–1510	60(30)[f]	
1068.2(2)	2640–1572	58(10)	
1112.85(10)	2623–1510	205(24)	$(E1)$
1163.8(2)	2137–973		

[a]Includes results from angular distribution and γ-γ coincidence measurements.
[b]Errors on the last digit are a combination of uncertainties coming from peak fitting and efficiency calibration of the spectrum.
[c]Relative gamma-ray transition intensities normalized to the 431 keV transition in ^{141}Pm. Errors on the last digit(s) are uncertainties in peak fitting and efficiency calibration.
[d]Multipolarities are obtained from the angular distribution coefficients presented in Table I.
[e]From the previous work of Refs. 5 and 6.
[f]Intensity estimated from coincidence data.

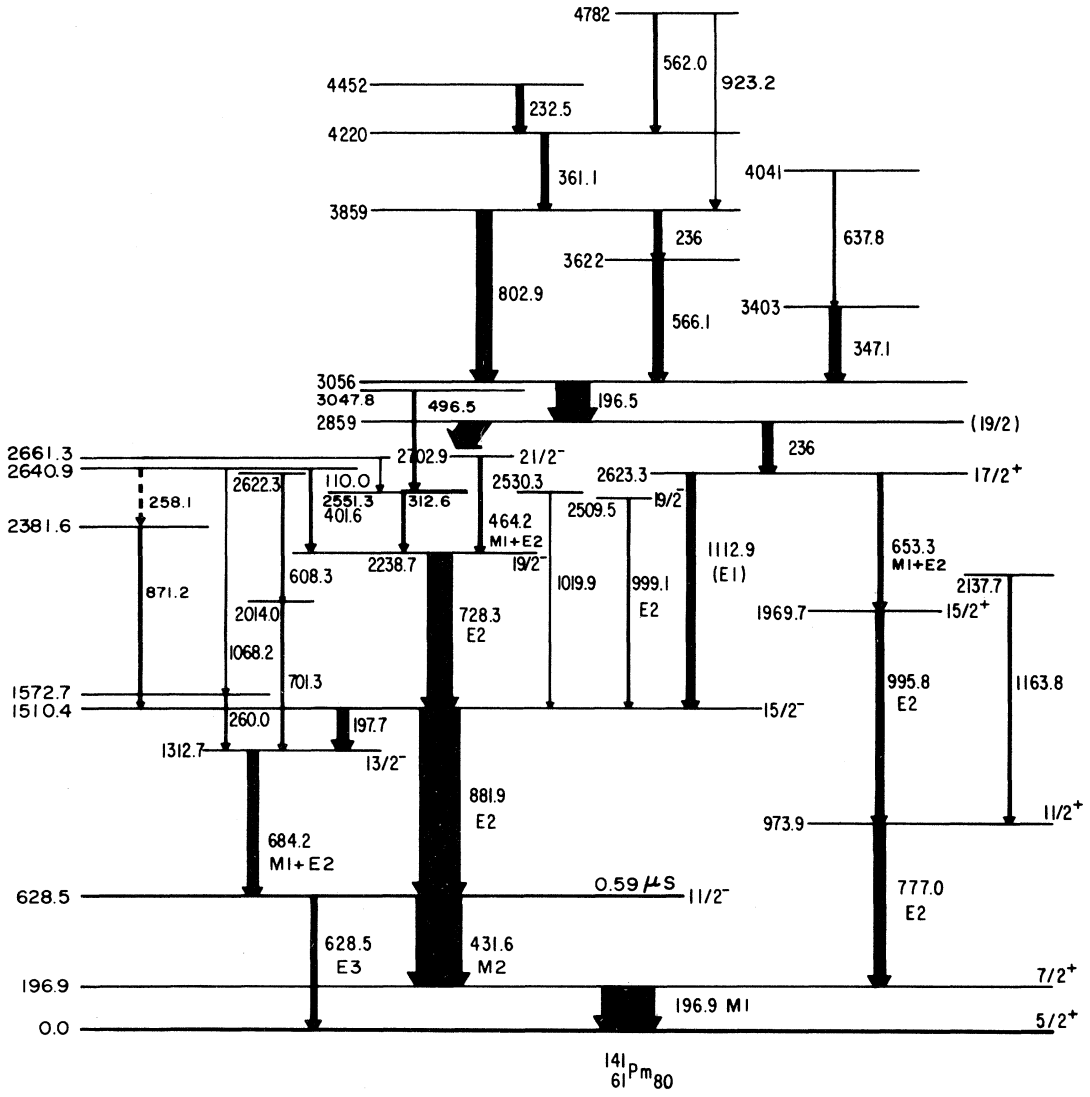

FIG. 5. The gamma-ray deexcitation scheme of ^{141}Pm obtained from the ^{126}Te(^{19}F,4$n\gamma$) reaction.

it should be placed above the 312 keV transition, but it is also in prompt coincidence with the 177 keV line, which is in between the 802 keV transition and the 728 and/or 881 keV transitions.

We also see some evidence for at least two more cascades feeding the 2238 keV level. One cascade includes the 169, 354, 682, and 951 keV lines and the other one includes the 254, 314, 461, and 651 keV lines. In all of these cases the relevant spectra did not have sufficient statistics to enable us to place these lines unambiguously.

IV. DISCUSSION

The $N=82$ nucleus ^{146}Gd has low-lying excitations characteristic of a doubly magic nucleus, supporting a large gap in the single-proton levels at the $Z=64$ subshell closure. This gap in the proton levels becomes less important as the number of valence neutrons increases: $N>88$ Gd nuclei have long been recognized as deformed, while more recent work[10] suggests that the $Z=64$ gap disappears for $N<78$. With two neutron holes in the shell below $N=82$ and three proton holes below $Z=64$, ^{141}Pm is then a good candidate for a transitational nucleus which could be studied in terms of either a spherical shell model or collective models. In fact, much of the low-lying structure of ^{141}Pm can be thought of as the single-particle excitations of a valence proton. The observation of single-particle excitations at similar energies in the neighboring nuclei, such as ^{143}Pm,[11] justifies this assumption. Therefore, the $\frac{5}{2}^+$ ground state, the $\frac{7}{2}^+$ state at 196.9 keV and the $\frac{11}{2}^-$ state at 628.5 keV can be best described as $\pi d_{5/2}^{-1}$, $\pi g_{7/2}^{-1}$, and $\pi h_{11/2}$ single proton states, respectively. Within the spherical shell model, the higher-lying states would be three-particle excitations, namely, one-proton, two-neutron hole excitations. In

principle, the excitation energies could be calculated by carrying out the necessary angular momentum algebra for coupling of three angular momenta and combining the residual interactions of two particle configurations.[12]

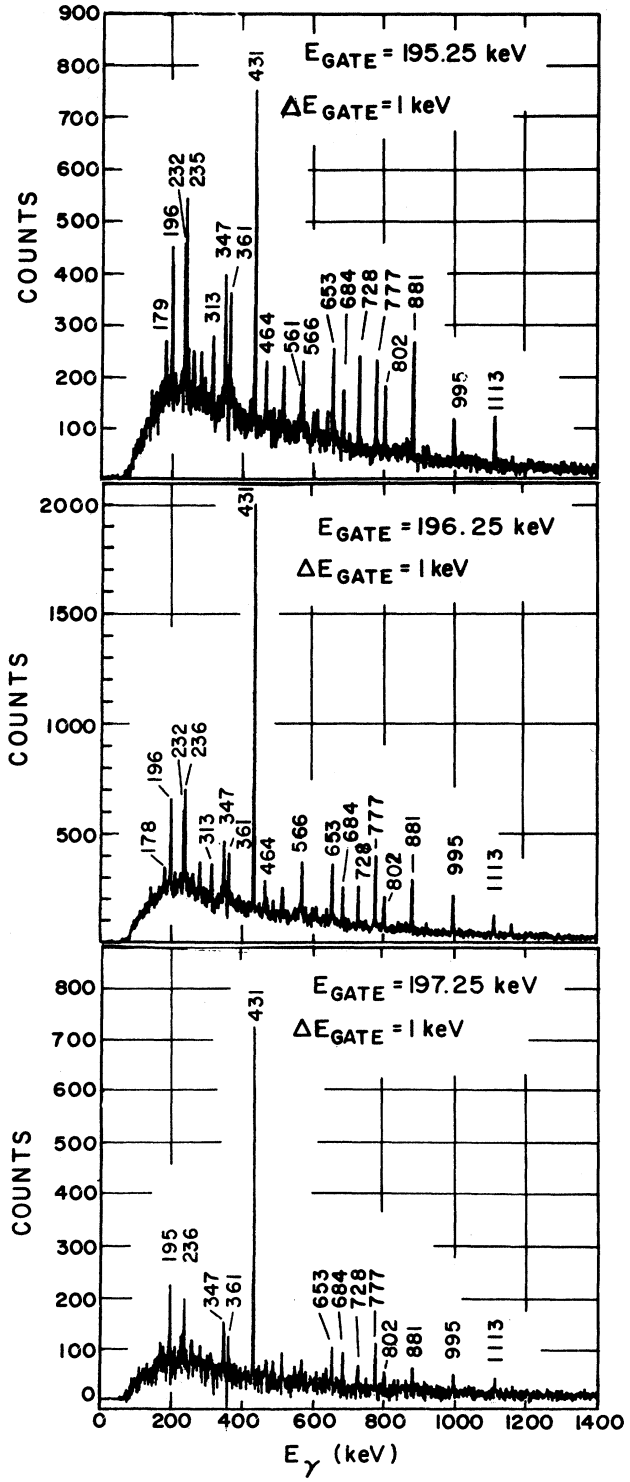

FIG. 6. Background subtracted γ-γ coincidence spectra obtained when gating on the lower energy, middle and higher energy portions of the 197 keV line.

However, empirical residual interaction energies for this region are not available and the neutron-proton interaction strengths, which would make it possible to calculate these residual interaction energies by using a modified surface delta interaction for a residual interaction,[12,13] are neither known nor easy to extract from the available data.

Piiparinen *et al.*,[5] and Aryaeinejad *et al.*,[6] have applied the triaxial rotor plus particle model of Meyer-ter-Vehn[14] to higher-energy excitations of the ^{141}Pm nucleus. In particular, the negative-parity levels above the $\frac{11}{2}^-$ isomeric state at 628.5 keV in ^{141}Pm were fitted by assuming that the valence $h_{11/2}$ proton is coupled to a triaxially deformed core with deformations $\beta=0.15$ and $\gamma=34°$. The triaxial rotor plus particle model calculations performed in the previous works[5,6] with these deformation parameters correctly reproduce the ordering of states in the $\pi h_{11/2}\otimes 2^+$ multiplet. However, Aryaeinejad *et al.*,[6] can not reproduce any higher-lying negative-parity states, including the yrast $\frac{19}{2}^-$ state which would be a pure $\pi h_{11/2}\otimes 4^+$ state in their model. In fact, the predictions of Ref. 6 are off by a few hundred keV for states above the $\frac{15}{2}^-$ state at 1510 keV. This poor agreement between experiment and theory may be because the states above the 2_1^+ state in the ^{140}Nd core are not collective.[3]

On the other hand, we can simply think of ^{141}Pm as a valence proton weakly coupled to the even-even core. Then we can estimate the centroid energies for the weakly coupled multiplets by adding the core excitation energies and the single-particle energies taken from the lower excited levels of ^{141}Pm. (Because we are taking the experimental excitation energies, these centroid estimates include the first-order perturbations for the weak coupling between the core and the single particle.) Centroid estimates for the negative-parity multiplets are compared with the experimental negative-parity levels in Fig. 7. Most of the negative-parity levels can be understood as an $h_{11/2}$ proton coupled to the ^{140}Nd core excitations. The lower $\frac{19}{2}^-$ state at 2238.7 keV was chosen as the member of the $4^+\otimes\pi h_{11/2}$ multiplet, instead of the $7^-\otimes\pi d_{5/2}$ multiplet, because of the relatively strong $E2$ transition between this $\frac{19}{2}^-$ state at 2238 keV and the $\frac{15}{2}^-$ state at 1510 keV. From our concurrent work,[3] we know that the 7^- state of the ^{140}Nd core is a two-neutron hole configuration, namely $(\nu h_{11/2}\nu d_{3/2})_{7^-}$, while the 4^+ state has a dominant proton configuration. Hence, the levels above the $2^+\otimes\pi h_{11/2}$ multiplet may be best described as three-particle excitations, instead of protons weakly coupled to collective core states.

In the same way, the low-lying positive-parity states can be best understood as $g_{7/2}$ and $d_{5/2}$ proton holes coupled to the ^{142}Sm core. The comparison of the experimental values to the calculated centroids for first-order coupling is given in Fig. 8. For the positive-parity states formed by coupling to the 2_1^+ state in the core, the identification of all of the members of this multiplet is not possible because of the density of the low-lying positive-parity states and the simplicity of our model. A candidate for the highest member of the $6^+\otimes\pi g_{7/2}^{-1}$ multiplet, namely the $\frac{19}{2}^+$ state, is observed above the $\frac{17}{2}^+$ state. If

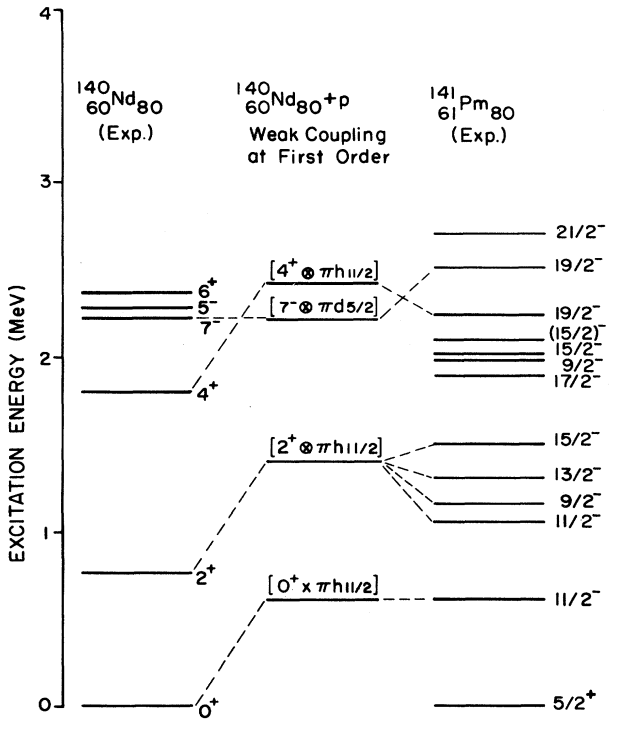

FIG. 7. Comparison of the centroid energies estimated for negative-parity multiplets and the experimentally established negative-parity states in ^{141}Pm. The data are taken from Refs. 5 and 6 and the present work.

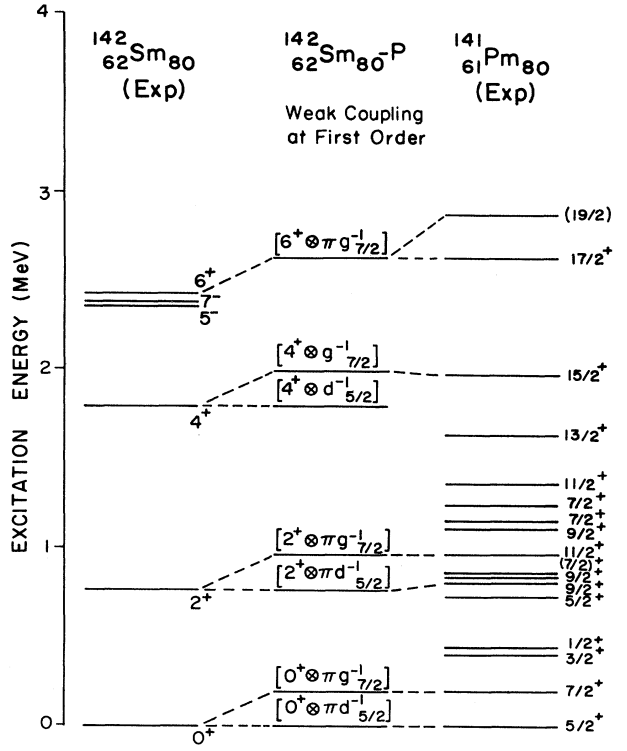

FIG. 8. Comparison of the centroid energies estimated for positive-parity multiplets and the experimentally established positive-parity states in ^{141}Pm. The data are taken from Refs. 5 and 6 and the present work.

the 6^+ of the core was a collective excitation, the aligned $\frac{19}{2}^+$ state would be the lowest lying member of the multiplet. However, the 6^+ core state is predominantly a two-proton excitation: a $(\pi g_{7/2}^{-2})_{6^+}$ configuration with a $(\pi g_{7/2}^{-1}\pi d_{5/2}^{-1})_{6^+}$ admixture.[3] Because of these π^2 constituents the $\frac{19}{2}^+$ state is not favored because of Pauli blocking.

V. CONCLUSIONS

The gamma-ray deexcitation of states in ^{141}Pm up to $E_x = 4782$ keV has been measured and a level spectrum obtained. The low-lying structure can be understood in terms of a simple weak-coupling picture of the valence proton in $d_{5/2}$, $g_{7/2}$, and $h_{11/2}$ orbitals. The higher-energy levels can be better described in terms of three particle configurations, given the two-particle nature of the core excitations.

This nucleus had previously been discussed[5,6] in terms of an $h_{11/2}$ proton coupled to a triaxial core. While previous work[6] was able to reproduce the ordering of the first $\pi h_{11/2} \otimes 2^+$ multiplet, rather poor agreement between experiment and theory was obtained for the states assigned to any higher multiplet. It is probably inappropriate to apply a collective model to $N = 80$ nuclei with few protons outside of the $Z = 64$ subshell closure. While the 2^+ states in the core nuclei may be collective (their excitation energies are considerably lower than can be calculated[3] with any single two particle configuration), the 4^+ and most definitely the 6^+ states in the $N = 80$ nuclei are *not* collective, but rather two proton configurations. The collectivity of the 2^+ states depresses their excitation relative to the 4^+ states, giving rise to an energy ratio $E(4^+)/E(2^+) \approx 2.3$, which would normally indicate a collective nucleus of transitional, possibly triaxial, character. However, this energy ratio is misleading, and should not be taken as a signature of vibrational or possibly triaxial shape. Rather the $N = 80$ nuclei near $Z = 64$ are of predominantly shell-model character; coupling a particle to the core will give rise to three-particle configurations, in agreement with our results presented in Figs. 7 and 8.

This work was supported in part by the U.S. Department of Energy under Contract No. DE-AC02-76ER03074.

*Present address: Department of Physics, University of California at Los Angeles, Los Angeles, CA 90024.
†Present address: Idaho National Engineering Laboratory, Idaho Falls, ID 83415.
‡Present address: Department of Physics and Astronomy, Rutgers University, New Brunswick, NJ 08903.

[1]C. J. Lister *et al.*, Phys. Rev. Lett. **55**, 810 (1985).
[2]G. A. Leander and P. Möller, Phys. Lett. **110B**, 810 (1982).
[3]E. Gülmez, H. Li, and J. A. Cizewski, Phys. Rev. C **36**, 2371 (1987).
[4]R. E. Epley, R. R. Todd, R. A. Warner, Wm. C. McHarris, and W. H. Kelly, Phys. Rev. C **5**, 1084 (1972); G. G. Kennedy, J. Deslauriers, S. C. Gujrathi, and S. K. Mar, Phys. Rev. C **15**, 792 (1977).
[5]M. Piiparinen, M. Kortelahti, A. Pakkanen, T. Komppa, and R. Komu, Nucl. Phys. **A343**, 57 (1980).
[6]R. Aryaeinejad, P. M. Walker, R. B. Firestone, and Wm. C. McHarris, Phys. Rev. C **32**, 1855 (1985).
[7]J. Becker, private communication.
[8]E. Gülmez, Ph.D. thesis, Yale University, 1986.
[9]E. Gülmez, M. W. Drigert, and J. A. Cizewski, Bull. Am. Phys. Soc. **31**, 836 (1986).
[10]J. A. Cizewski and E. Gülmez, Phys. Lett. B **175**, 11 (1986).
[11]T. Ishimatsu, H. Ohmura, T. Awaya, T. Nakagawa, H. Orihara, and K. Yagi, J. Phys. Soc. Jpn. **28**, 291 (1970).
[12]R. D. Lawson, *Theory of the Nuclear Shell Model* (Oxford University, New York, 1980).
[13]P. W. M. Glaudemans, B. H. Wildenthal, and J. B. McGrory, Phys. Lett. **21**, 427 (1966); P. W. M. Glaudemans, P. J. Brussard, and B. H. Wildenthal, Nucl. Phys. **A102**, 593 (1967).
[14]J. Meyer-ter-Vehn, Nucl. Phys. **A249**, 111 (1975); **A249**, 141 (1975).